Performance characteristics of the new Keck Observatory echelle spectrograph and imager

A.I. Sheinis[1], J. Miller[1] , M. Bolte[1], B. Sutin[2]

1. UCO/Lick Observatory, University of California, Santa Cruz, Kerr Hall, Santa Cruz, CA 95064

Phone: (831) 459-3581

Fax (831) 426-3115

2) Carnegie Observatories 813 Santa Barbara Street Pasadena, California 91101

Phone: (626) 577-1122

Fax: (626) 795-8136

The Echelle Spectrograph and Imager (ESI) is a multipurpose instrument which has been delivered by the Instrument Development Laboratory of Lick Observatory for use at the Cassegrain focus of the Keck II telescope. ESI saw first light on August 29, 1999. The optical performance of the instrument has been measured using artificial calibration sources and starlight. Measurements of the average image FWHM in echelle mode are 22 microns (0.22 arcseconds), 16 to 18 microns (0.16 to 0.18 arcseconds) in broad band imaging mode, and comparable in the low-dispersion prismatic mode (LDP). Images on the sky, under best seeing conditions show FWHM sizes of 34 microns (0.34 arcseconds). Maximum efficiencies are measured to be 30% for echelle and anticipated to be greater than 38% for low dispersion prismatic mode including atmospheric, telescope and detector losses. In this paper we describe the instrument and its specifications. We discuss the testing that led to the above conclusions.

Keywords: spectrograph, imager, echelle, Keck, astronomy

1. Introduction

The Echelle Spectrograph and Imager (ESI) is the most recently commissioned instrument at the Keck Observatory. ESI was built at the Instrument Development Laboratory of UCO/Lick Observatory. It is a multi-purpose imaging spectrograph used the Cassegrain focus of the Keck II telescope.

ESI can be quickly switched between three modes. In echelle mode ten orders that cover 0.39 to 1.10 microns with no spectral gaps are imaged onto the single

2048x4096 pixel detector. The echelle mode uses a slit length of 20 arcseconds and dispersion ranging from 0.15 A/pixel (order 15 in the blue) to 0.39 A/pixel (order 6 in the red). The low-dispersion prismatic mode (LDP) is a very efficient prism-dispersed spectrum with dispersion ranging from 0.75 A/pixel at 4000A to 10 A/pixel at 10000A. A slit up to 8 arcmin-long or multi-slits can be used in this mode. The final configuration is direct imaging with a rectangular field 2 x 8 arcmin and 0.153 arcsec/pixel delivered to the CCD. The design and initial tests suggest ESI should deliver the best image quality of any of the Keck optical instruments.

2. Scientific Rationale

The principal niche envisioned for ESI was very high-throughput medium-resolution optical spectroscopy with wide wavelength coverage in a single exposure. Examples of the science programs that drove the choice of resolution are internal kinematic and abundance studies of distance galaxies, detailed abundance determinations for stars as faint as V=22 (which includes the bright giants in Local Group galaxies) and

absorption-line studies in the line-of-sight to QSOs. The low-dispersion/multiobject and direct imaging capabilities were added after the echelle design was conceptualized. In the low-dispersion mode, this is likely the most powerful spectrograph in operation for obtaining low-resolution spectra of extremely faint objects. Redshift information and spectral energy distributions for very faint galaxies or low-luminosity stars in the Galaxy should be possible to V>25.

The third mode of ESI is direct imaging capability over a moderate sized (2’ x 8’) field. Narrow band imaging capability; will be used to study the spatial distribution of ionized gas (H , [OII], [OIII]) and the nature of star formation in distant galaxies, or the host galaxies of QSO’s, for example.

3. Instrument description

3.1 Overview of Specifications and Operating Modes

Specifications for the overall design and the three operating modes are described below.

Instrument Specifications

Wavelength coverage: 3900 - 11000 Å

Collimated beam diameter: 160 mm

Collimator focal length: 2.29 m

Grating: Milton-Roy, 175 lines/mm, 32.3 degree blaze angle

Prisms: BSL7Y, 50.00 degree apex angles

Camera: Refracting, 10 all-spherical elements

Camera focal length: 308 mm

CCD: 2K x 4K, 15 micron pixels (identical to DEIMOS chip)

Mode 1: Echelle in near-Littrow configuration

The medium resolution mode uses a catalogue echelle grating, and two prism cross-dispersers, one of which is used in double-pass to provide pre-dispersion. Table 1 shows diffraction orders, wavelength ranges, and dispersions for the echelle mode.

Resolution: 11.4 km/sec/pixel average

Spectral coverage: 3900-11000 A, no gaps, in a single exposure

Pixel size on the sky: 0.153 arc-sec in dispersion direction, 0.15 +/- 25% in slit direction

(due to prism anamorphic distortion.)

Single grating in fixed position

Two prisms, one used in double pass (pre-dispersion)

Order spacing: 20 arc-sec minimum, echelle orders 6 - 15

Mode 2: High Efficiency, low dispersion configuration

The high efficiency mode bypasses the grating by inserting a flat mirror behind the pre-disperser prism.

Dispersion: variable; from 60 to 350 km/sec/pixel

Spectral coverage: 3900-11000 Å in a single exposure

Throughput: up to 45 % including detector (for "fresh" telescope coatings)

Multi-slit mode: 10 - 50 objects using slit masks

Mode 3: Direct imaging configuration

The direct imaging mode bypasses the grating and the prisms by inserting a flat mirror ahead of the pre-disperser prism, and by retracting the second prism from the optical axis.

Field shape: rectangular

Field size: 2 x 8 arc-min

Pixel size on the sky: 0.153 arc-sec

Collimated beam: 160 mm

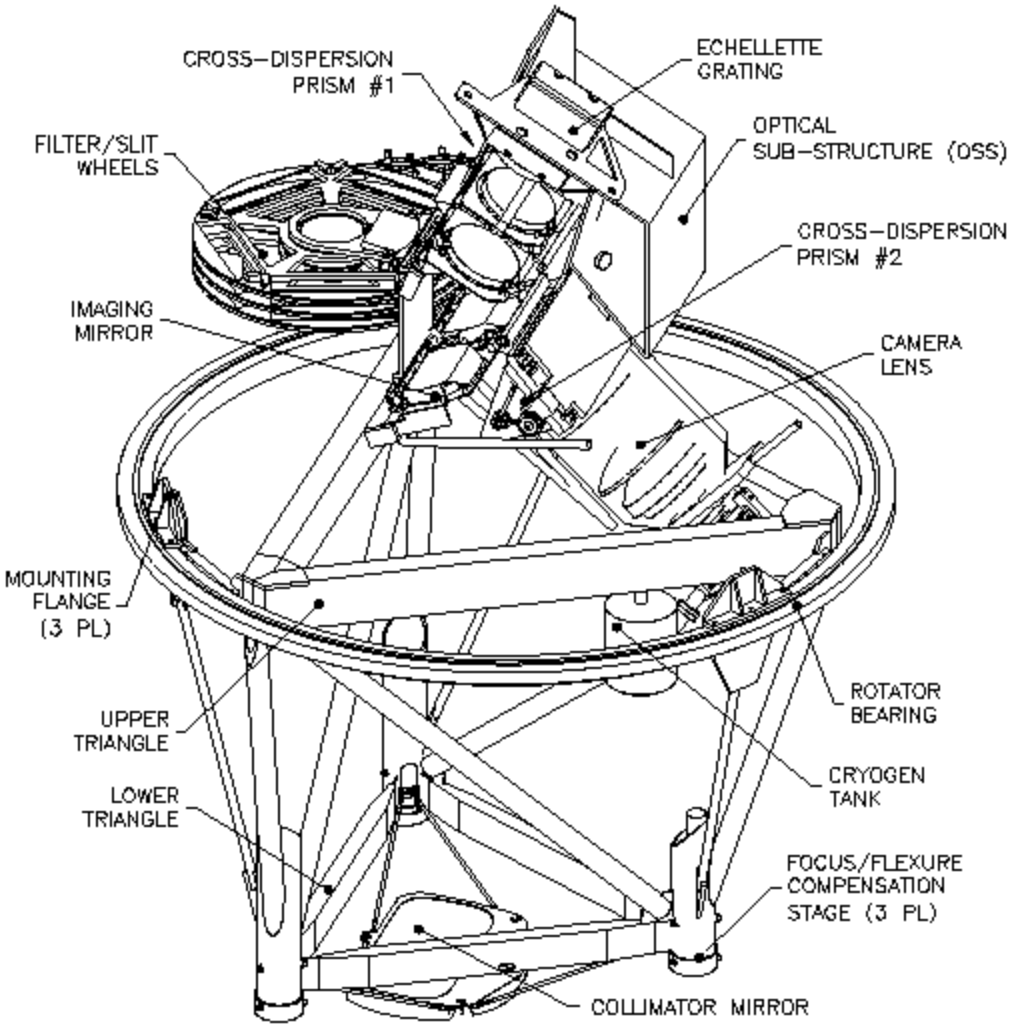

Figure 1, ESI Configuration

^M

3.2 Optical design

Harland Epps (UCO/Lick Observatory) created the optical design of the camera. It consists of ten lens elements in five lens groups. The camera has an effective focal length of 308 mm. It has an entrance aperture diameter of 287 mm and a final plate scale of 97.7 microns/arcsec on the sky. The collimated beam diameter is approximately 160 mm. The camera’s effective f/ratio in imaging mode is thus

f/1.93 and slightly faster in spectroscopic modes due to anamorphism.

The camera design is all-spherical and it includes two large CaF_2 lenses. Group #1 is a doublet, group #2 is a CaF_2 singlet, groups #3 and #4 are triplets while group #5 is the field flattener/dewar window. The elements in groups #1 and #3 are optically coupled with a fluid (Cargille laser liquid Type 5610 n(D)=1.5000) to minimize internal reflections. The elements in group #4 are greased together with Dow Corning Q2-3067 optical couplant.. Broad passband AR coatings were applied on all optics. The camera is described in detail in Epps 1998[9] and Sheinis et al 1999[10] .

The ESI optical design is complicated by the fact that a wide variety of pupil anamorphic factors and effective entrance pupil distances are presented to the camera's entrance aperture by reason of the three operating modes. In practice, the camera design was slightly compromised in the imaging and LDP modes so as to favor the echelle mode. Nevertheless, the echelle mode remains the most severe test of system image quality.

One of the authors (B.S.) optimized the optical design of the spectrograph. The spectrograph has a fixed 175.6 line/mm echelle grating from Milton Roy (now Spectronics, Rochester, NY 14625) and two large (25 kg) cross-dispersion prisms made of BSL7Y glass from Ohara Corp., (San Clemente, CA). The prisms were polished by Zygo (Middlefield, CT) and coated with multi-layer dielectric anti-reflection coatings (AR) by Coherent Inc., (Auburn, CA). ESI also contains a reflective collimator, which is an off-axis segment of an on-axis ellipsoid, figured by TORC, (Tucson, AZ) and coated by Newport Thin Films Laboratory, (Chico, CA). The spectrograph optical system is described in detail in Sutin 1998[8].

To create the low dispersion mode, a fold mirror is translated into the beam before the grating. The fold mirror redirects the beam to the prisms, bypassing the grating. In this way, the beam is only dispersed by the prisms. To create the imaging mode another fold mirror is inserted into the beam before the prisms, bypassing both the grating and the prisms. In this way the beam is passed directly to the camera without being dispersed . The prism and mirror mechanisms are described in detail in Sheinis[3] et al 1998 and Sheinis[13] et al 1999.

3.3 Detector and Controller

The ESI detector is an MIT/Lincoln Labs CCID20 CCD[13] with 4096 rows and 2048 columns of 15 micron square pixels. Measured deviations from flatness at room temperature are ~ +/- 2 microns. The on-chip amplifier read noise is measured to be ~ 2.7 electrons. The charge transfer efficiency (CTE) was measured to be 0.999998 per pixel transfer in both serial register and the imaging array. The controller for ESI is a San Diego Sate University second-generation device(SDSU2) developed by Robert Leach [14] **.**

4. Predicted System Performance

The theoretical system performance is described in considerable detail by Sutin[8]. For this analysis he used the pre-construction ESI camera Run No. 2990 (02/27/96) by Epps[9]. The system analysis was done on an in-house lens design code written by Sutin.

Spot sizes

The system performance was calculated using the final as-built camera Run No. 102297AC. Orders 6 in the infrared through 15 in the blue were ray-traced at five wavelengths uniformly spaced over each free-spectral range without refocus. The $_{rms}$ spot-size diameter (D_{rms}) was calculated for each image. Averaging these image diameters over all wavelengths and all orders the Ave($_{rms}$) = 19.0 +/- 3.3 microns. The corresponding 80% encircled ray diameter average is Ave(80%) = 22.5 +/- 4.2 microns, while Ave(90%) = 28.4 +/- 5.6 microns. RMS spot sizes at the center of each order are shown for all orders in table 1.

Table 1 Predicted Performance, Echelle Mode

ORDER	Wavelength range (microns)	center D_{rms} (microns)	center D_{rms} (Arcsecs)	A/pix
15	0.393 –0.419	12.01	0.122502	0.15
14	0.420 – 0.451	16.03	0.163506	
13	0.451 – 0.486	19.58	0.199716	0.18
12	0.487 – 0.529	19.15	0.19533	0.19
11	0.529 – 0.581	17.2	0.17544	0.21
10	0.581 – 0.640	17.86	0.182172	0.23
9	0.640 – 0.715	22.24	0.226848	0.26
8	0.715 – 0.813	25.46	0.259692	0.29
7	0.813 – 0.937	24.19	0.246738	0.33
6	0.937 – 1.093	15.93	0.162486	0.39

Table 2 shows the predicted RMS spot diameters for a central field point and a range of wavelengths. Table 3 shows the predicted RMS spot diameters for several field points with no imaging filter in place i.e band pass of 0.39 – 1.1 microns.

Table 2 Predicted Performance, LDP Mode

Lambda microns	location(X)	Location(Y)	D_{rms} (microns)	D_{rms} (arcsecs)
0.39	0.06124	0.52395	11.67	0.119034
0.46	-0.01969	0.1533	28.15	0.28713
0.53	0.0043	-0.06002	21.1	0.21522
0.6	0.01991	-0.19864	13.23	0.134946
0.67	0.03095	-0.29646	12.14	0.123828
0.74	0.03929	-0.37034	13.75	0.14025
0.81	0.04595	-0.42931	13.63	0.139026
0.88	0.05152	-0.47862	11.53	0.117606
0.95	0.05636	-0.52148	10.74	0.109548
1.02	0.0607	-0.55997	16.64	0.169728
1.09	0.06472	-0.59552	28.71	0.292842

Table 3 Predicted Performance, Imaging Mode

Field point X(arcmin)	Field point Y(acrmin)	chip location(X)	Chip Location(Y)	D_{rms} (microns)	D_{rms} (arcsecs)
0	0	-0.03248	0.26339	18.87	0.192474
1	0.5	-0.24756	0.12224	19.47	0.198594
2	1	-0.46281	-0.01888	22.18	0.226236

3	1	-0.69145	-0.04562	27.47	0.280194
4	1	-0.92016	-0.07224	33.19	0.338538

5. Measured System Performance

5.1 Camera Bench Testing and Performance Analysis

After laboratory assembly of the camera, a battery of optical performance tests, including interferometric testing, polychromatic point spread function measurement and back focal distance measurement were carried out. The results of these tests were then compared to the predictions from the lens design. These tests are discussed in detail in the literature [10]. For example, the polychromatic (Wratten 54) RMS spot diameter on-axis was measured to be 13.7 microns.

5.2. Artificial-source testing

After assembly and integration into the Keck II telescope a series of optical tests was performed to assess the optical performance of the instrument. In the imaging mode, optical performance was analyzed by imaging an array of pinholes placed in the slit mask location. In the LDP mode a linear array of pinholes was used and in the echelle mode a single pinhole was used. The pinholes are 125 microns in diameter, which projects to 16.8 microns at the detector (compared to 15 micron pixels). Thus they contribute slightly to convolved spot sizes. The pinholes were illuminated by either the dome floodlamps or by the internal quartz-halogen flat lamp. The case of dome illumination most accurately mimics the star illumination as the Keck II pupil is imaged into ESI. In the case of internal flat field lamps internal baffles become the system stop. These apertures are larger than the Keck pupil and not hexagonal. Thus the artificial source tests overestimate the image sizes due to overfilling of the camera pupil. For the case of imaging mode the standard filter set provided with ESI (Johnson B & V, and Spinrad R and Gunn I) and no-filter were used. In all cases a series of images was taken at a range of focus settings.

Image quality was determined by fitting each spot to a two dimensional azimuthally averaged gaussian distribution using Information Data Language (IDL), (Research Systems Boulder CO). The radial profiling routine returns the standard deviation for each fitted gaussain. These were converted to the two dimensional RMS spot diameters (D_{rms}) by multiplying the standard deviation by 2.828. D_{rms} was determined for a variety of wavelengths as a function of focal position in the two spectroscopic modes. In the imaging mode D_{rms} was

determined for a variety of field positions as a function of focal position. These data are plotted in figure 2. The D_{rms} values in this plot were computed as the median over location on the chip of the D_{rms} values as a function of camera focal position.

The D_{rms} at best focus is compared to that predicted for the design in table 4. The data in table 4 show a discrepancy between design prediction and measured Drms. This discrepancy is not consistent with the laboratory testing of the camera alone, which agreed well with the design prediction. We believe this discrepancy is due in part to fabrication and assembly errors, and in part to the improper illumination in the testing, as mentioned above. Additional testing is required to differentiate between these two possibilities. Two sets of tests are planned which include night sky illumination of a pinhole mask in Echelle and LDP mode and line-lamp illumination of a pinhole mask via the dome in Echelle and LDP mode. These tests will further isolate the spectrograph from seeing and telescope related optical limitations. We will report the results in a later paper.

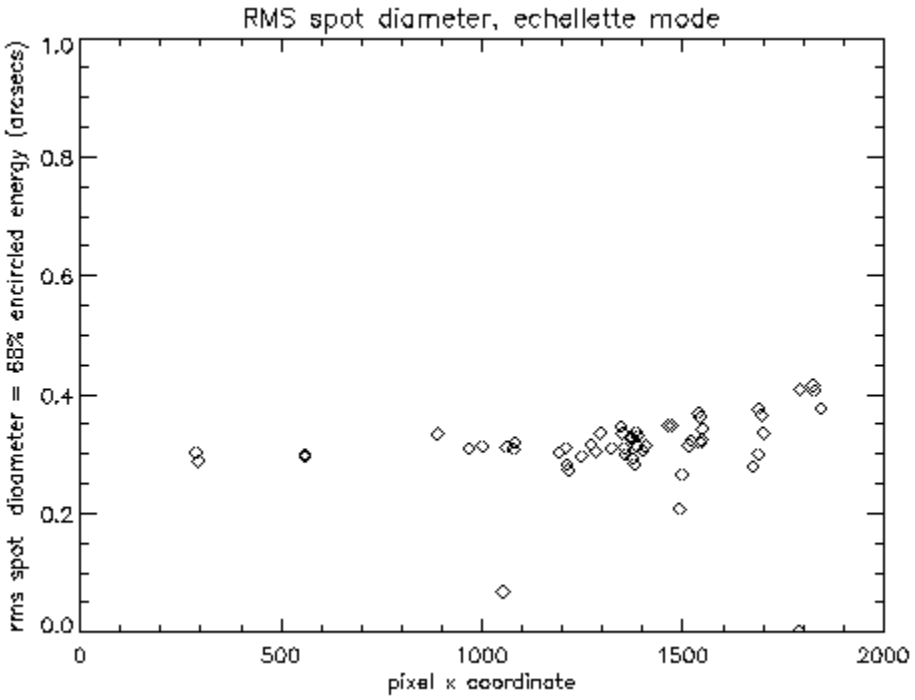

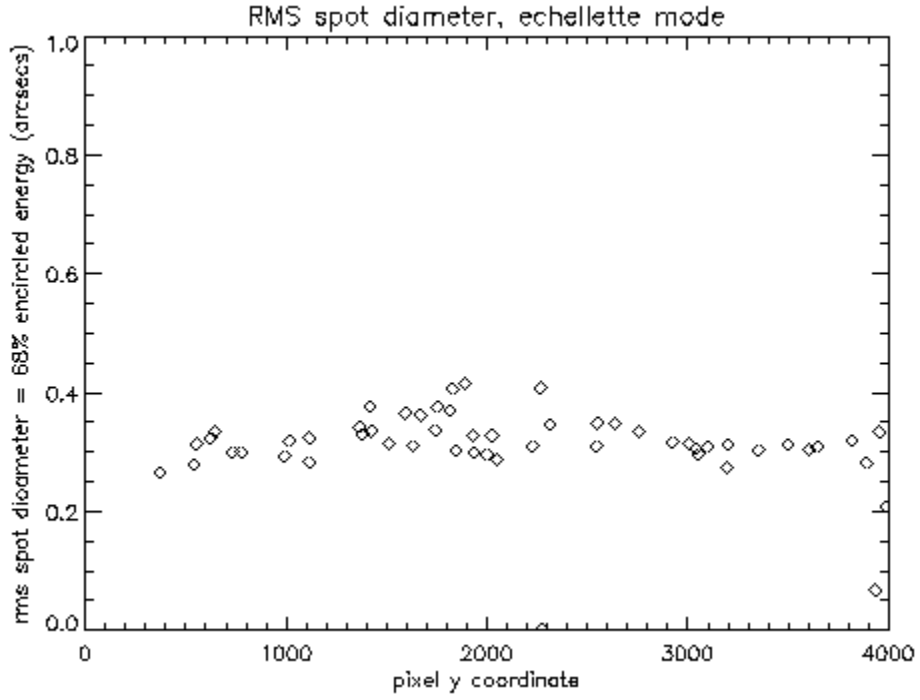

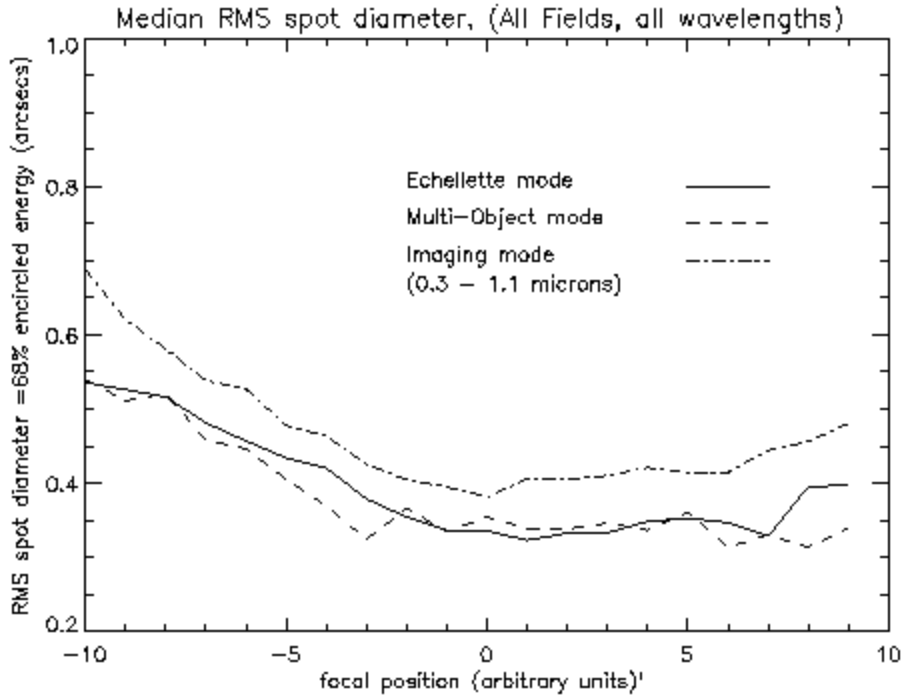

Table 4: Median rms spot Diameters

	Measured	D_{rms}	design	D_{rms}	Illumination
	Microns	arcsecs	microns	arcsecs	Internal

Echelle	31.7	0.32	19	0.19	Internal
LDP	30.8	0.31	16	0.16	Internal
Imaging (no filter)	37.4	0.38	24	0.25	Internal
JohnsonB	20.7	0.21	11.7	0.12	Dome
JohnsonV	22.3	0.22	13.3	0.13	Dome
Spinrad R	23.6	0.24	15.2	0.15	Dome
Gunn I	23.6	0.24	15.6	0.16	Dome

Figures 3 and 4 show D_{rms} as a function of position on the chip for the echelle mode. The uniformity of the spot size as a function of location is an indication that the field curvature and chip tilt are negligible

5.4 performance on the sky

Several globular clusters were observed in BVRI, under good seeing conditions. The FWHM was calculated for each image using the IRAF image reduction package. This was done by fitting the azimuthally averaged images to gaussian energy distributions. The quality of the fit and the FWHM of the fitted images for the I band are displayed in figure 5.

The average R and I band images have a FWHM of 0.34 arcsecs. The B and V band images are slightly larger. The R and I band image size is consistent with the best FWHM seeing disk of 0.28 arcsecs convolved with an average instrument FWHM of 0.18 arcsecs assuming no guiding errors. These are the best non-AO optical images at Keck to date.

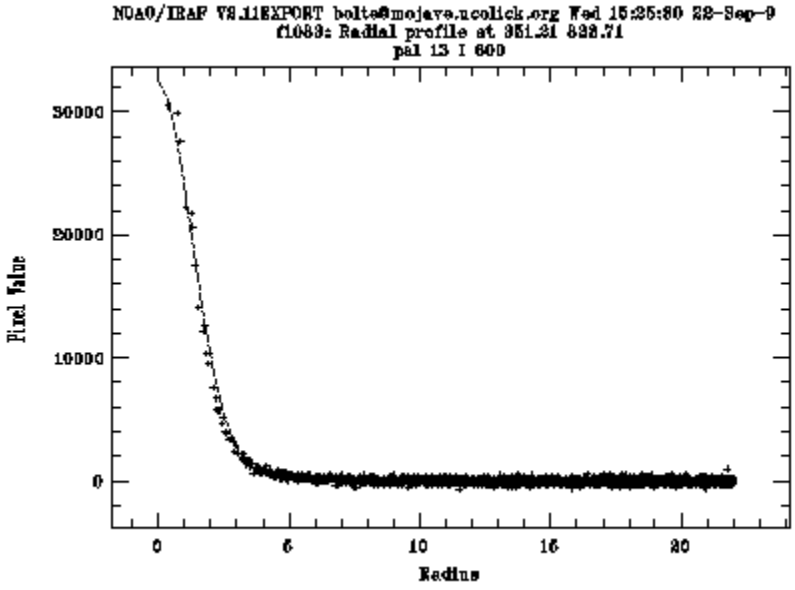
NOAO/IRAF V8.11EXPORT bolte@mojave.ucolick.org Wed 15:25:30 22-Sep-9
f1083: Radial profile at 351.21 822.71
pal 13 I 600
30000
20000
10000
0
Pixel Value
0
5
10
15
20
Radius

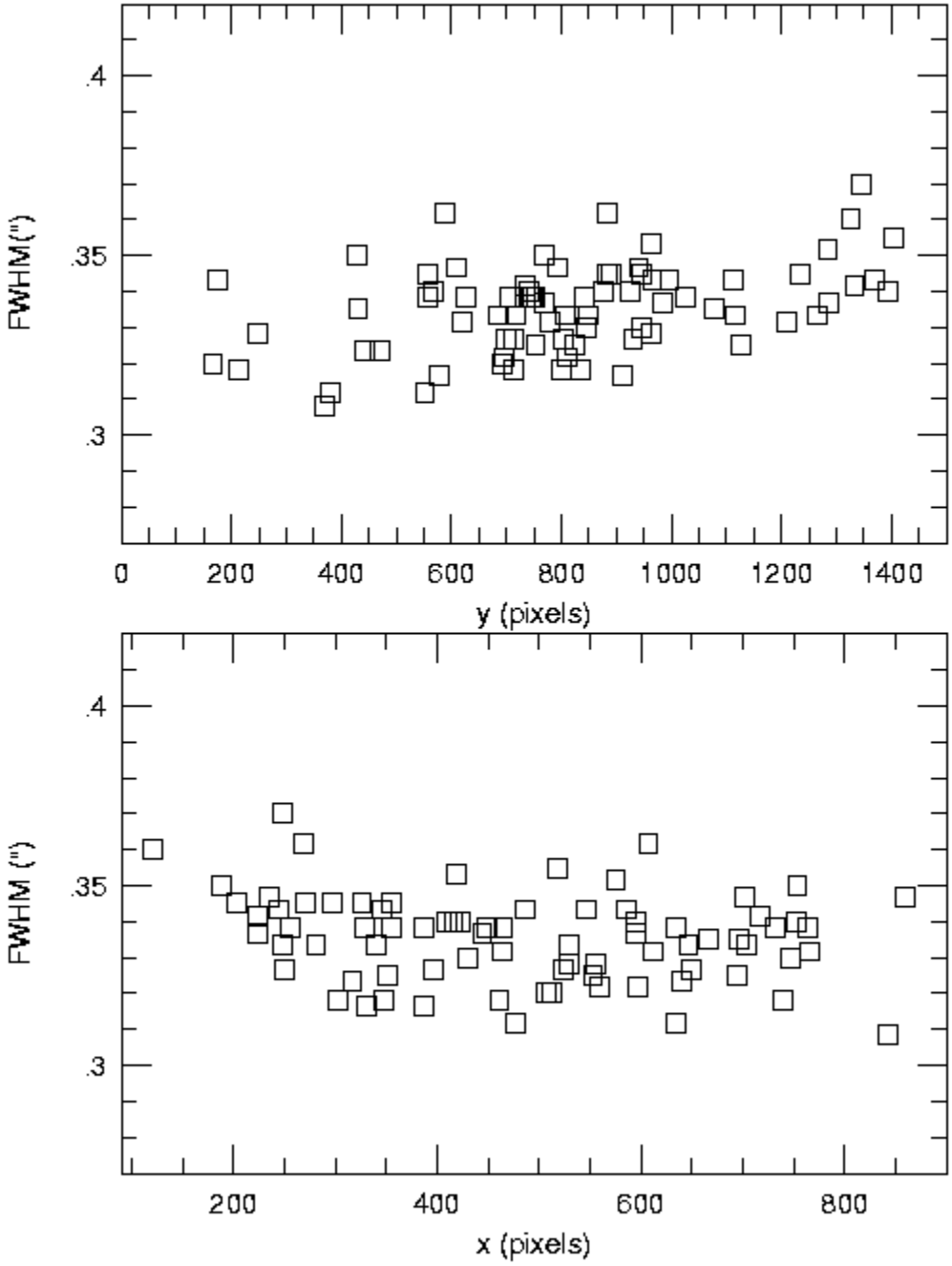

6. Efficiency

6.1 Instrument Efficiency in Echelle Mode

Observations of the spectrophotometric standard Wolf 1348 were made through a

6"-wide slit during the September 1999 commissioning run. The observations were corrected for an airmass of 1.04 using the mean extinction curve for Mauna Kea downloaded from the Canada-France-Hawaii WWW site. The values for flux/wavelength for Wolf 1348 were taken from the tables Massey[15, 16] and converted into photons per second per angstrom using the relation:

$$N_l = 4.275 \times 10^{12}/l \times 10^{-(m_l + A_l X)/2.5}$$

Here m_l is the magnitude from the Massey et. al.[15, 16] tables, A_l is the extinction at l in magnitudes per angstrom and X is the airmass of the observation.

Table 3 gives the ratio of the number of photons predicted for Wolf 1348 to the number detected (corrected to the top of the atmosphere). The first efficiency is for the telescope, instrument plus slit losses, the second assumes the "fresh" aluminum efficiency curves for two mirrors (the primary and secondary). These numbers have been calculated order by order (that is not summing the flux at a given wavelength that is detected in more than one order) and the values in the table are at the peak efficiency of each order. For the bluer orders, adding flux from adjacent orders at a common wavelength increases the overall throughput at some wavelengths by as much as 60%

Table 5: Instrument Efficiency, echellette mode

Order number	**l_{peak}**	**Al**	**Eff. #1 (%)**	**Eff. #2 (%)**
15	4178	0.315	11	15
14	4450	0.250	16	22
13	4750	0.204	19	25
12	5150	0.167	23	30
11	5625	0.147	28	36
10	6150	0.125	26	33

9	6850	0.081	26	34
8	7550	0.061	22	30
7	8650	0.045	17	23
6				

6.1 Instrument Efficiency in LDP Mode:

The efficiency in LDP mode is expected to be at least 20 % better than echelle as the beam in this mode is common path except for the grating. A fold mirror replaces the grating in the LDP mode. The fold mirror has an enhanced silver coating with reflectance approaching 99%. The efficiency of grating is at best 80% and typically worse. Using these numbers we expect a peak efficiency of the LDP mode, including telescope, atmospheric and detector losses to be greater than 35 % with average telescope transmission and greater than 45% with freshly coated telescope mirrors.

7.Conclusion

We have discussed the optical imaging performance of the ESI spectrograph in terms of throughput, image sizes and field flatness. This has been done both for test images on artificial objects, and images of astronomical objects. Image quality has been shown to be superb in all three modes, with measured image FWHM sizes in Johnson B and V, Spinrad R, and Gunn I bands of 16.2, 17.4, 18.4 and 18.4 microns respectively. Imaging studies of globular clusters have produced the best visible images to date at Keck observatory.

Throughput of the instrument and telescope (including detector) in echellette mode has been tested to be up to 28% and estimated to be greater than 35% in LDP mode with average telescope mirror coatings.

8. Acknowledgments

The authors wish to thank Harland Epps, Jerry Nelson, Terry Mast, Matt Radovan and Jack Osborne for their many helpful comments. We would also like to thank Bob Goodrich and the staff at Keck Observatory for their help with the assembly, testing and data acquisition for this instrument.

9. Bibliography

1. Epps, H., and Miller, J., "Echelle Spectrograph and Imager for Keck Observatory," *Proc. SPIE* **3355**, pp. 48-58, March 1998
2. Sutin,B., "What an optical designer can do for you AFTER you get the design," *Proc. SPIE* **3355**, pp. 134-143, March 1998
3. Sheinis, A.I., et al., " Large prism mounting to minimize rotation in Cassegrain instruments," *Proc. SPIE* **3355**, pp. 59-69, March 1998
4. Radovan, M. V. ,et al., "Design of a collimator support to provide flexure control on Cassegrain spectrographs," *Proc. SPIE* **3355**, pp. 155-163, March 1998
5. Bigelow, B.C., and Nelson, J.E., "Determinate space-frame structure for the Keck II echelle spectrograph and imager (ESI)," *Proc. SPIE* **3355**, pp. 164-174, March 1998
6. Hilyard, D., "Chemical Reactivity Testing of Optical Fluids and Materials in the DEIMOS Spectrographic Camera for the Keck II Telescope," *Proc. SPIE* **3786**, July 1999
7. Oke, J.B. et al., "The Keck Low-Resolution Imaging Spectrometer," **PASP 107**, pp. 375-385, April 1995
8. Sutin,B., "ESI: a new spectrograph for the Keck II telescope," *Proc. SPIE* **2871**, pp. 1116-1125, June 1996
9. Epps, H., "Development of large high-performance lenses for astronomical spectrographs," *Proc. SPIE* **3355**, pp. 111-128**,** March 1998
10. Sheinis, A.I., et al., "Assembly and testing of the ESI camera," *Proc. SPIE* **3786**, July 1999
11. Bigelow, B. C. and Nelson J.E., "Determinate space-frame structure for the Keck II echelle spectrograph and imager (ESI)" *Proc. SPIE* **3355**, March 1998
12. Sheinis, A.I., et al., "Kinematic Translation Mechanism for Moderate-Sized Optics" *Proc. SPIE* **3786**, July 1999
13. Burke, B.E., et al., "Large are, back illuminated CCD imager development" *ESO Conference on CCD Detector Technology for Astronomy,* Garching, in press, Oct 1996
14. Leach, R. W., "CCD Controller requirements for ground-based astronomy", *Solid State Sensor Arrays and CCD Cameras*, *Proc. SPIE* **3355**, March 1998
15. Massey, P., Strobel, K., Barnes, J. V. & Anderson, E. 1988, ApJ, 328, 315.
16. Massey, P. & Gronwall, C., 1990, ApJ, 348, 344